J Mater Sci: Mater Med (2013) 24:1491–1499
DOI 10.1007/s10856-013-4900-y

Synthesis of hybrid sol–gel materials and their biological evaluation with human mesenchymal stem cells

M. Hernández-Escolano · M. J. Juan-Díaz · M. Martínez-Ibáñez · J. Suay · I. Goñi · M. Gurruchaga

Received: 19 June 2012 / Accepted: 21 February 2013 / Published online: 9 March 2013
© Springer Science+Business Media New York 2013

Abstract Surface engineering of biomaterials could promote the osseointegration of implants. In this work, two types of hybrid sol–gel materials were developed to stimulate cell attachment, proliferation and differentiation of osteogenic cells. One type was synthesised from vinyl triethoxysilane (VTES) and tetraethyl-orthosilicate (TEOS) at different molar ratios, while the other from VTES and hydroxyapatite particles (HAp). Hybrid materials were systematically investigated using nuclear magnetic resonance, Fourier transform infrared spectroscopy and contact angle metrology. The biocompatibility and osseoinduction of the coatings were evaluated by measuring mesenchymal stem cell proliferation using MTT assays and analysing the mineralised extracellular matrix production by quantifying calcium-rich deposits. The results highlighted the versatility of these coatings in obtaining different properties by changing the molar ratio of the VTES:TEOS precursors. Thus, mineralisation was stimulated by increasing TEOS content, while the addition of HAp improved cell proliferation but worsened mineralisation.

M. Hernández-Escolano (✉)
Centro de Biomateriales e Ingeniería Tisular, Universidad Politécnica de Valencia, C. de Vera s/n, 46021 Valencia, Spain
e-mail: miriam.hernandez.escolano@gmail.com
URL: http://www.upv.es/cb/

M. J. Juan-Díaz · M. Martínez-Ibáñez · I. Goñi · M. Gurruchaga
Facultad de Ciencias Químicas, Universidad del País Vasco, P. M de Lardizábal, 3, 20018 San Sebastián, Spain

J. Suay
Dep. Ingeniería de Sistemas Industriales y Diseño, Universidad de Castellón, Av. Sos Baynat s/n, 12071 Castellón, Spain

1 Introduction

It is well known that the biological response induced by a biomaterial is directly related to its surface characteristics. Physicochemical factors such as surface roughness, wettability and surface energy, as well as chemical composition, among others, determine this response. Generally, middle hydrophilic surfaces allow interactions with biological fluids, cells and tissues. Moreover, materials with high surface energy and acidity increase osteoblastic differentiation [1].

Among the cell types involved in bone regeneration are mesenchymal stem cells (MSCs) [2]. When attached onto the surface of prostheses, they can drastically accelerate the integration of the implant [3]. Thus, there is great interest in the successful culturing of such cells. It is important to recall that cells cannot interact directly with the biomaterial, but need a protein to achieve the interaction. This protein is needed for recognition by the integrins on cell surfaces, which then trigger specific signalling pathways related to attachment, proliferation and mineralisation. Therefore, adsorption of proteins onto the implant surface is influenced by the chemical composition, mechanical and physical properties and topography of the prosthesis [4–6].

Consequently, it is important to improve the surface properties of implants in order to develop substrates that stimulate the osseointegration process. Surface engineering (the application of organic, inorganic or hybrid coatings) can promote osseointegration of the implants, making them amenable to osteogenic cell proliferation and differentiation, thus stimulating bone regeneration [7–13].

An interesting technique to prepare coatings is the sol–gel method, which is a wet chemical process. This technique can be used to obtain a wide range of coatings: metallic oxide glass, bioceramic, bioactive titania-like

surfaces and hybrid organic–inorganic coatings, among others [14, 15]. Biological applications of sol–gel materials have been extensively studied during the past decade [16, 17], proving their efficiency as biomaterials due to their unique features. First, sol–gel coatings protect against efficacious corrosion induced by different substrates [8, 18, 19]. From a biological point of view, these coatings present Si–OH groups that promote the precipitation of biomimetic hydroxyapatite, which is essential for the osseointegration of the implant [20, 21]. Moreover, the degradation of these coatings releases silanols into the cellular environment, which assists in regenerating new bone [20–24]. Finally, sol–gel coatings can be obtained by choosing different precursors, giving rise to surfaces with a range of wettability values, degradation rates or functional groups [25]. Moreover, due to this high versatility, they can be loaded with biomolecules such as peptides, proteins and drugs.

In this study, two sets of organic–inorganic hybrid coatings were obtained by the sol–gel technique. The first set was prepared from vinyl triethoxysilane (VTES) and tetraethyl-orthosilicate (TEOS) using various molar ratios to obtain materials with different wettabilities. The second set was obtained from VTES doped with particles of hydroxyapatite as a promoter of nucleation of biomimetic hydroxyapatite [26, 27]. Furthermore, systematic analysis of the material network formation, chemical composition and wettability of the thin films was performed. Finally, the effect of these coatings on the proliferation of human MSCs was investigated.

2 Materials and methods

2.1 Sol–gel film preparation

2.1.1 Substrate preparation

Glass Petri dishes (18 mm in diameter, Afora) were used as the substrate for sol–gel deposition. The glass Petri dishes were cleaned in an ethanol bath, ultrasonicated for 5 min at a power of 30 w using a Sonoplus HD 3200, rinsed in distilled water, soaked in ethanol and, finally, dried at 150 °C. Afterwards, to improve wettability, the glass Petri dishes were activated by an Argon plasma treatment (200 sccm) for 30 s (PLASMA-ELECTRONIC PICCOLO, 50 Pa, 300 W).

2.1.2 Sol–gel synthesis and deposition

Organic–inorganic hybrid coatings were synthesised from VTES (Sigma-Aldrich) and TEOS (Sigma-Aldrich). The molar ratios were 1:0, 9:1, 8:2 and 7:3 (VTES:TEOS). In all cases, 2-propanol was used as the co-solvent to obtain a miscible solution of the siloxanes, the volume ratio alcohol:siloxane was defined as 1:1 and the stoichiometric amount of acidified water was used as the catalyst of the reaction. The acidified water was prepared by mixing distilled water with 0.1 N HNO_3 until a pH of 1 was achieved. Solutions were stirred for about 1 h and left for another hour at room temperature before their deposition onto the Petri dishes by solving casting. These 2 h were necessary to ensure the hydrolysis of all the ethoxy groups.

Bioactive organic–inorganic hybrids were synthesised from VTES using the same protocol described above. In this case, a dispersion of hydroxyapatite particles (size >200 nm Sigma-Aldrich) in 2-propanol was added to the sol at concentrations of 2.5 and 5 w/w (weight of HAp per total weight of silanes) at the end of the hydrolysis reaction.

To obtain a homogenous coating of the glass surface, a drop of a 10 µl sol was flowed horizontally. The thermal curing of the coatings was optimised until homogeneous films, free of cracks and transparent, were obtained. The thermal process applied is described in Table 1.

2.2 Network formation

The chemical characterisation of the network formation was carried out using Fourier transform infrared spectroscopy (FTIR, Thermo Nicolet NEXUS, 4,000–500 cm^{-1} wavelength range) in the ATR mode and solid-state silicon nuclear magnetic resonance spectroscopy (^{29}Si-NMR, Bruker 400 AVANCE II).

To observe the reaction progress, liquid-state ^{29}Si-NMR was used. The spectra were recorded on a Bruker 400 AVANCE II spectrophotometer. Samples were prepared by adding chromium acetylacetonate to the reaction medium as a spin relaxation agent at a concentration of 2.5×10^{-3} M, to overcome the long relaxation times [24]. Tetramethylsilane was used as the internal reference.

2.3 Contact angle measurements

Wettability of the coatings was determined by the sessile drop method. Contact angles were measured using an OCA20 Goniometer. Deionised water was used as the probe liquid. A sessile drop of 10 µl was placed on the coating surface. The value given was the mean value of at least 10 measurements.

2.4 Degradability

Hydrolytic degradation was evaluated by measuring weight loss of the samples before and after soaking in phosphate buffered saline (PBS), pH 7.4, at 37 °C. The PBS was

Table 1 Conditions of thermal curing applied to the various materials

Material	VTES*	V:T	V + HAp[a]
Curing temperature (°C)	100	50	100
Curing time (min)	90	120	90

[a] After curing, the samples were dried at 50 °C for 15 min and set the final temperature at 3 °C/min

made from $NaH_2PO_4 \cdot H_2O$ (Sigma-Aldrich) and $Na_2HPO_4 \cdot 7H_2O$ (Panreac). In this case, the samples were prepared on a non-adherent substrate. These samples had a final thickness of around 1 mm. After soaking, the samples were dried in an oven at 37 °C for 24 h.

2.5 Assays with MSCs

The biocompatibility and osteoinduction of the coatings were tested with adult MSCs (AMSCs). To perform cell culture on the samples, the sol–gel coatings were sterilised by exposure to UV for 30 min in a tissue culture cabin. All samples were preconditioned by overnight dipping in Dulbecco's modified Eagle's medium (DMEM-Glutamax) (Gibco) to ensure protein adsorption.

To perform cell adhesion and proliferation assays, about 47,500 cells/well were seeded onto the sample surfaces and incubated for 14 days at 37 °C in 5 % CO_2/air atmosphere. Cell proliferation was measured by analysing mitochondrial activity using a colorimetric cell proliferation test kit (MTT, Roche) at different culture times (0, 7 and 14 days). Absorbance was measured with a Multiskan Ascent at $\lambda = 550$ nm. The experiments were performed in triplicate.

To analyse the osteoinduction capacity of the coatings, the calcium-rich deposits formed by cells in an osteogenic culture medium were measured using Alizarin Red S staining. To perform the assay, about 7,600 cells/well were seeded onto the surface and incubated in DMEM-Glutamax containing 10 % foetal bovine serum (FBS) for 7 days at 37 °C in 5 % CO_2/air atmosphere. Then, the culture medium was replaced by Osteoblast Differentiation medium (Gibco) and incubated for a further 14 days, changing the medium every 72–96 h. Finally, the calcium-rich deposits were quantified using 2 % Alizarin Red (Sigma-Aldrich), pH 4.1–4.3. Absorbance was measured with a Multiskan Ascent at $\lambda = 570$ nm.

2.6 Statistical analysis

Statistical analysis was performed using the one-way ANOVA technique. The error protection method used in this research was the Fisher PLSD method and the confidence limit used was 95 %.

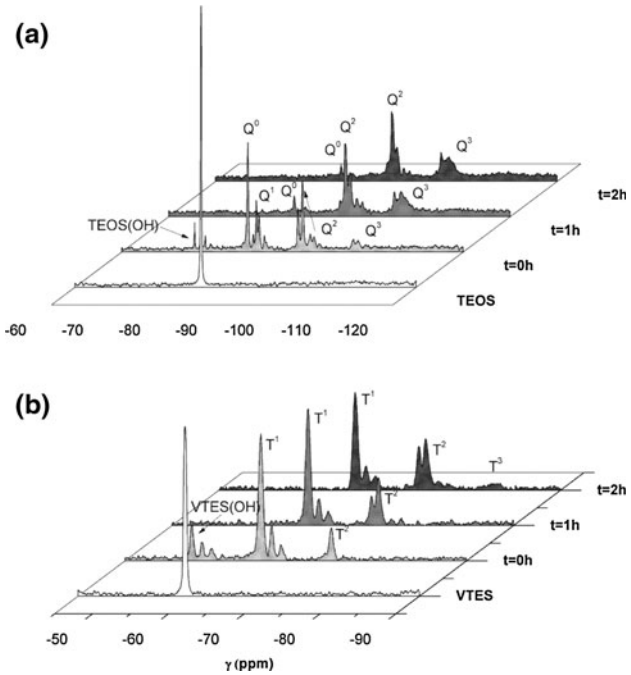

Fig. 1 **a** Liquid-state ^{29}Si-NMR spectra of TEOS and **b** VTES

3 Results

3.1 Network formation

In all cases, a continuous film free of cracks and defects was obtained. However, films containing HA showed a surface roughness due to the lack of solubility of HA in the reaction medium. The films kept the integrity during handling for tests and measurements, suggesting a good crosslinking degree. Liquid NMR spectroscopy showed the formation of condensed species in all the cases (Figs. 1, 2), being TEOS the alkoxysilane that promotes the crosslinking in a highest extend. These results were corroborated by solid NMR spectroscopy (Fig. 3) and FTIR.

3.2 Wettability of the coatings

Sol–gel coatings presented contact angle values slightly lower than 90°. The measurements range from 75.8 ± 1.2 to 82.3 ± 0.7, and all of them had a statistically significant

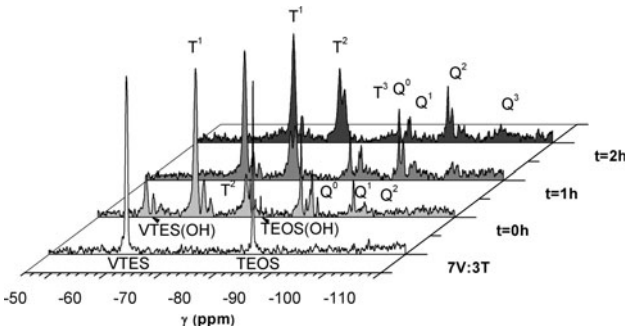

Fig. 2 Liquid-state ^{29}Si-NMR spectra of the VTES:TEOS molar ratio 7:3

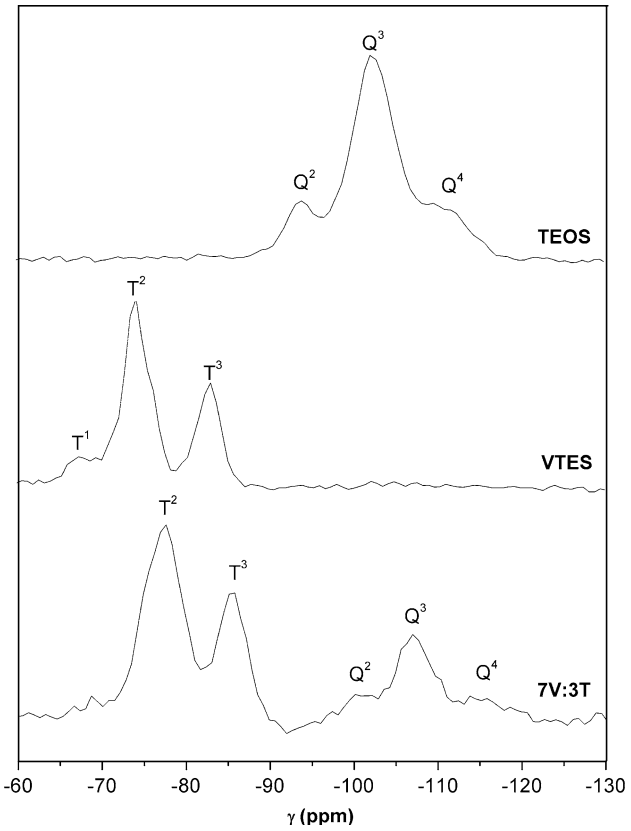

Fig. 3 Solid-state ^{29}Si-NMR spectra of VTES:TEOS at a molar ratio of 7:3

difference with the contact angle of pure VTES films (ANOVA $p \leq 0.05$)

Contact angles for all the samples (Table 2) were higher than that of the control (glass). The coated samples became more hydrophilic with increasing TEOS molar ratios; thus, the coating with a VTES:TEOS molar ratio of 7:3 was the most hydrophilic. When adding different amounts of HAp particles to the VTES coating, the contact angle increased, obtaining the highest value with 2.5 % of HAp.

3.3 Degradability of the material

The material made from VTES had a low degradation ratio, showing a value (Table 3) of nearly 3 % in 7 days that remained the same after 21 days. The weight loss in the material with added TEOS was higher even after 7 days. After 21 days of soaking, the loss increased with increasing levels of TEOS. The weight loss of all the coatings showed a statistically significant difference with that of pure VTES films in both periods (ANOVA $p \leq 0.05$)

3.4 Biological evaluation

Comparisons of AMSC attachment and proliferation among the various coatings (Fig. 4), identified the materials formulated with TEOS and HAp addition as undergoing significant in vitro changes compared with pure VTES. As the quantity of TEOS increased, the values of absorbance grew slightly. The detected mitochondrial activity at the initial culture time was five times higher for coatings containing HAp. However, the amount of HAp added to the material did not elicit significant differences in cell proliferation.

The production of mineralised extracellular matrix on the different coatings (Fig. 5) determined that the addition of TEOS improved the mineralisation, although there were no significant differences among the samples with different TEOS molar ratios. On VTES surfaces, the number of calcium deposits decreased on day 14, but for coatings with VTES + 2.5 % of HAp and 5 % of HAp, this number increased during the assay days of culturing.

4 Discussion

Today, an important part of the research to enhance metallic implants osseointegration is focussed on the fixation of coatings of different characteristics to the implant surface. Many works proposed HAp coatings and in many cases, silicon-containing HAp is used [28, 29] There are also a few papers in which the authors developed sol–gel coatings based in alkoxysilanes. Some of them demonstrated a good in vitro performance with an enhancement of the proliferation of osteoblast cells [30, 31]. However, most of them studied the techniques to obtain different surfaces or the influence of the incorporation of different elements in the coating formulation, more than the influence of all the features involved in the biological performance, as in this paper. As explained in the introduction, the obtaining of films containing Si, capable to coat metallic implants, could be interesting to improve the osseointegration of such implants [22–24]. Various different organic–inorganic hybrid coatings have been synthesized in this work by

means of the sol–gel method. First, the condensation and curing processes were optimised studying the evolution of the Si–O–Si bonds formation through ^{29}Si-NMR spectroscopy, solid and liquid. The spectra obtained revealed a faster condensation rate for TEOS siloxane than for VTES. This is attributed to the presence of the vinyl group, which provide to the molecule with a big and hydrophobic moiety that hinder both the hydrolysis and condensation reactions. This trend is kept in the formulations with both siloxanes.

Table 2 Contact angle measurements for uncoated (glass) and coated samples at different molar ratios of VTES:TEOS or different levels of HAp

Formulation	Wetting contact angle (°)
Glass	28.3 ± 0.2
VTES	78.9 ± 0.5
VTES + 2.5 % HAp	82.3 ± 0.7*
VTES + 5 % HAp	80.6 ± 1.2*
9V:1T	78.0 ± 1.0*
8V:2T	78.0 ± 0.6*
7V:3T	75.8 ± 1.2*

Statistical analysis was carried out using an ANOVA ($p \leq 0.05$)

* Statistically significant difference in values between samples and VTES

Table 3 Hydrolytic degradation (weight loss) at 37 °C in PBS for VTES, 9V:1T, 8V:2T and 7V:3T on days 7 and 21

Coating composition	Weight loss (%)	
	7 days	21 days
VTES	2.67 ± 0.78	3.33 ± 0.09
9V:1T	12.97 ± 0.01	16.98 ± 0.77
8V:2T	11.18 ± 0.84	17.53 ± 0.09
7V:3T	12.34 ± 1.13	19.78 ± 0.37

4.1 Films optimization

The formation of the sol–gel network depends on the condensation reaction of the Si–OH (obtained by the initial hydrolysis of the alkoxysilanes) to form Si–O–Si bonds. Depending on the extent of the reaction, networks with different degrees of crosslinking are obtained. In this study, we tried to synthesise sol–gel coatings with the maximum condensation degree. Thus, a previous study of the hydrolysis and condensation process was necessary.

The hydrolysis process was followed up by liquid-state ^{29}Si-NMR spectroscopy. To have a reference, the spectra corresponding to both alkoxysilane precursors dissolved in 2-propanol were first recorded. Afterwards, a stoichiometric amount of acidified water was added to the NMR sample tubes and new spectra were recorded every hour until no changes were observed. The nomenclature followed was the one described widely in the literature [25–27]. T character was used for VTES followed by a superscript ranging from 0 to 3, and Q was used for TEOS followed by a superscript ranging from 0 to 4, depending on the number of oxygen atoms with which condensation with another silicon atom has occurred.

Figure 1a shows the spectra of TEOS in isopropanol and reaction medium during the hydrolysis/condensation reactions. The spectrum of TEOS had a single signal at −82 ppm. However, once the acidified water was added, a peak corresponding to hydrolysed moieties appeared at −72 ppm. Moreover, Q^1, Q^2 and Q^3 peaks could already be observed, although an important fraction of the precursor (Q^0) remained unreacted. One hour later, the peaks

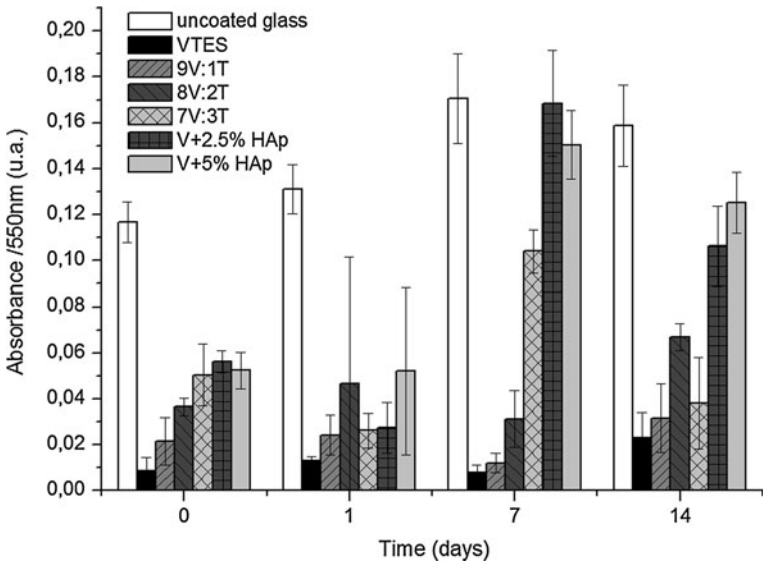

Fig. 4 AMSC proliferation curves on uncoated glass and coating surfaces (VTES, 9V:1T, 8V:2T, 7V:3T, VTES + 2.5 %HAp and VTES + 5 %HAp). Absorbance was measured at 550 nm

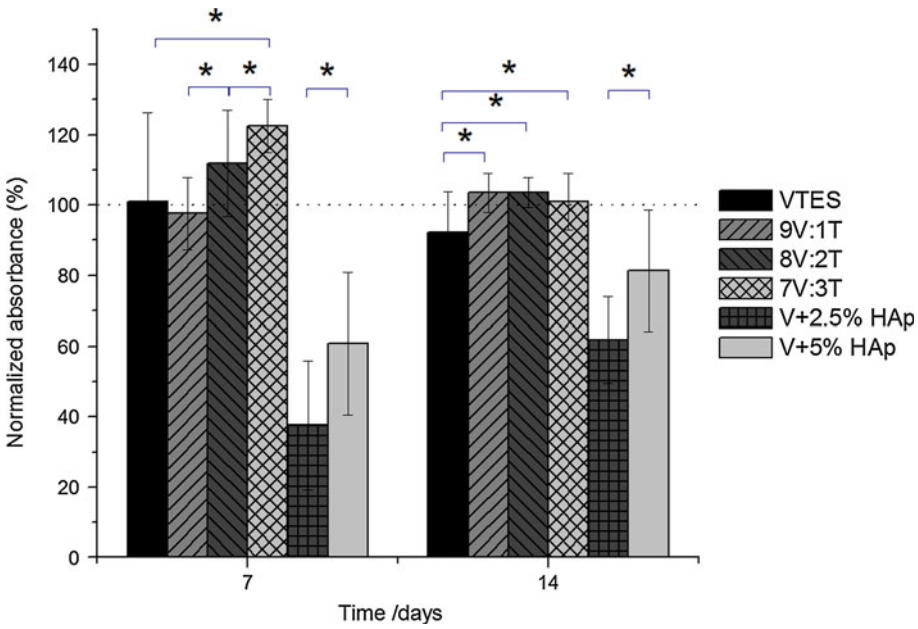

Fig. 5 Quantification of mineralisation by analysing calcium-rich deposits in osteogenic cultures using Alizarin Red S staining on coating surfaces (VTES, 9V:1T, 8V:2T, 7V:3T, VTES + 2.5 %HAp and VTES + 5 %HAp). Values were normalised against those of the glass control. Statistical analysis was carried out using an ANOVA ($p \leq 0.05$). *Statistically significant difference in values between samples

attributed to hydrolysed TEOS and Q^1 disappeared, whilst the shift corresponding to Q^0 decreased considerably and the intensity of the peaks corresponding to Q^2 and Q^3 increased. After 2 h, a slight change was observed in the spectrum: Q^0 decreased again while the signals associated with the more condensed species, Q^2 and Q^3, increased. Nevertheless, the progress of the reaction did not undergo a very noticeable change.

Spectra corresponding to reactions with VTES are presented in Fig. 1b. The Si shift of the precursor dissolved in isopropanol was found at −59 ppm. Peaks corresponding to hydrolysed moieties and the condensed groups T^1 and T^2 were detected as soon as the acidified water was added. As the reaction progressed, the signal of the silanol groups disappeared and T^1 and T^2 increased. At 2 h, a signal type T^3 was observed, indicating that the condensation was advancing. In this case, T^0 disappeared at the very moment the acidified water was added.

Figure 2 shows the spectra of the 7:3 VTES:TEOS molar ratio. The spectra for 9:1 and 8:2 VTES:TEOS molar ratios were also recorded, but the changes during the reaction process were similar enough in all three cases to choose only one ratio for representation. The Si shift corresponding to VTES and TEOS occurred at −59 and −72 ppm, respectively. From the first moment of adding the acidified water, peaks corresponding to hydrolysed moieties could be detected, together with those of the condensed groups, i.e., T^1, T^2, Q^1 and Q^2. As the reaction progressed, the signals of the silanol groups disappeared, those of T^1, T^2, Q^1 and Q^2 increased, and T^3 and Q^3 signals appeared (Table 4), indicating that the condensation was advancing. At 2 h of reaction, no significant changes were registered. Similar to when TEOS was condensed alone, the Q^0 signal decreased during the reaction, but could be observed during the entire process. All the peaks of these spectra split to cover a broader shift due to the condensation among the species coming from both precursors and the less condensed moieties.

VTES and 7V:3T films were also studied by solid-state ^{29}Si-NMR after the condensation treatment (Fig. 3). Although TEOS did not give rise to a film, a solid material was obtained after a curing treatment at 50 °C for 1 h, which was used to generate a spectrum for comparative purposes. Thus, the solid-state ^{29}Si-NMR spectrum of the TEOS coating showed signals associated with Q^2, Q^3 and Q^4. The intensity ratios of these signals indicated a higher number of the Q^3 species. The VTES coating spectrum showed T^1, T^2 and T^3 signals, showing higher intensity in T^2 than in T^3. After the curing treatment of sample 7V:3T, the T^3 and Q^4 species appeared. Those signals did not appear in the liquid NMR spectrum, thus they determined a progress of the condensation process, as expected. The broader signals observed in this spectrum were due to the combined condensation of both precursors. Additionally, the signals corresponding to the less condensed species (T^1, Q^1) and Q^2 disappeared (Table 5).

FTIR spectroscopy corroborated NMR findings and was very useful to prove the presence of the vinyl group after the curing. Thus, the coatings will contain a reactive group, which would offer a functionalized surface for biocompatibility purposes. Furthermore, depending on VTES/TEOS ratio we could obtain surfaces with different hydrophobicity degree and functional groups amount, which would affect to the biocompatibility.

A detailed study by FTIR of 7V:3T sample generated relevant information concerning the composition of the

Table 4 ^{29}Si chemical shift of the VTES:TEOS sample with the 7:3 ratio in liquid form

7V:3T	^{29}Si chemical shift δ (ppm)								
	OH	T^0	T^1	T^2	T^3	Q^0	Q^1	Q^2	Q^3
VTES	−53	−59	−62	−71	−82		–	–	–
TEOS	−81	–	–	–	–	−81	−82	−91	−100

Table 5 ^{29}Si chemical shift in solid samples of TEOS, VTES and 7:3 VTES:TEOS

	^{29}Si chemical shift δ (ppm)					
	T^1	T^2	T^3	Q^2	Q^3	Q^4
TEOS	–	–	–	−93	−102	−109
VTES	−67	−74	−82	–	–	–
7V:3T						
TEOS	–	–	–	−100	−107	−113
VTES	–	−77	−85	–	–	–

coatings. The spectrum showed the presence of two bands (1,075 and 1,163 cm^{-1}), assigned to the asymmetric vibration of the oxygen atoms in the Si–O–Si group [32, 33]. Moreover, it presented a band due to the symmetric vibration of the Si–O–Si bonds in the 700–800 cm^{-1} region. Those bands were characteristics of the network formation [32, 33]. The characteristic OH band (3,800–3,300 cm^{-1}) was assigned to residual ethanol and water from the sol–gel reactions. The band near 3,740 cm^{-1} was assigned to the stretching vibration of structural OH groups corresponding to unreacted terminal Si–OH groups [32, 33]. The characteristic bands associated with the vinyl group were also detected (=CH_2: 3,060 cm^{-1}; C=C: 1,600 cm^{-1}). The bond between the organic chain and the inorganic network, Si–C, produced a signal at 1,450 cm^{-1} [34].

4.2 Biological behavior evaluation

It is well known that Si–O–Si networks can be hydrolytically degraded, giving rise to Si–OH groups that form $Si(OH)_4$ soluble compounds [35]. We can observe that the degradation was strongly improved with the addition of TEOS. Obviously, the breakage of Si–O–Si bonds should be easier in the absence of hydrophobic organic groups (i.e. vinyl groups). Therefore, as the molar ratio of TEOS increases, the ratio of inorganic to organic material increases, consequently enhancing the degradability of the coating and hence the Si release. Since Si compounds are described as stimulators of osteoblastic differentiation [20–24], the role of the degradation process of the coatings is important in order to relate it to cell behaviour. Actually, at the sight of the biological tests results, we could say that the presence of TEOS clearly increases the mesenchymal cells proliferation, probably due to the more hydrophilic character of TEOS containing coatings. Additionally, the formulations of VTES with HAp showed the highest proliferation values. In this case, the roughness of the surface obtained by the addition of HAp nanoparticles could be the responsible for the cell growth increase [36]. However, the behaviour of the various coatings in the Alizarin Red staining test showed a different tendency. On the one hand, the presence of TEOS caused a slight enhancement of the mineralisation as a consequence of the Si release after the degradation. On the other, the addition of HAp produced the lowest degree of calcium rich deposits. This could be due to the crystallinity of the HAp used in this work, which was not sufficient to enhance mineralisation. A similar behaviour has been reported in the literature when using various HAp types with Ti and other materials [37, 38].

5 Conclusions

Sol–gel is a promising method of obtaining osteoinductive surfaces and versatile materials that can be optimised to achieve the desired properties. The wettability and degradation rate of the samples could be controlled by changing the VTES:TEOS molar ratio, while TEOS addition increased the water contact angle and hydrolytic degradation. In line with these results, it was possible to enhance AMSC attachment and differentiation by adding TEOS to VTES coatings, which improved the degradability of the films and mineralised extracellular matrix production. HAp–VTES coatings gave better cell attachment and proliferation results, but there was no improvement in

osteoinduction. For that reason, further formulations are currently being studied.

Acknowledgments The supports of the Spanish Ministry of Economy and Competitiveness through project IPT-010000-2010-004, the University of the Basque Country (UPV/EHU) through "UFI11/56" and the Basque Government though the program for Grupos Consolidados IT-234-07 are kindly acknowledged. We are especially thankful to D. Antonio Coso and the personal of his company (Ilerimplant S.L. www.ilerimplant.com) for their cooperation.

References

1. Le Guéhennec L, Soueidan A, Layrolle P, Amouriq Y. Surface treatments of titanium dental implants for rapid osseointegration. Dent Mater. 2007;23(7):844–54.
2. Bruder SP, Caplan AI. Bone regeneration through cellular engineering. In: Lanza RP, Langer R, Vacanti J, editors. Principles of tissue engineering. 2nd ed. San Diego: Academic Press; 2000. p. 683–96.
3. Manso M, Ogueta S, Herrero-Fernández P, Vázquez L, Langlet M, García-Ruiz JP. Biological evaluation of aerosol–gel-derived hydroxyapatite coatings with human mesenchymal stem cells. Biomaterials. 2002;23(19):3985–90.
4. Choi AH, Ben-Nissan B. Sol–gel production of bioactive nanocoatings for medical applications. Part II: current research and development. Nanomedicine. 2007;2(1):51–61. doi:10.2217/17435889.2.1.51.
5. Anselme K, Linez P, Bigerelle M, Le Maguer D, Le Maguer A, Hardouin P, Hildebrand HF, Iost A, Leroy JM. The relative influence of the topography and chemistry of $TiAl_6V_4$ surfaces on osteoblastic cell behaviour. Biomaterials. 2000;21(15):1567–77.
6. Amaral M, Lopes MA, Santos JD, Silva RF. Wettability and surface charge of Si_3N_4–bioglass composites in contact with simulated physiological liquids. Biomaterials. 2002;23(20):4123–9.
7. Paital SR, Dahotre NB. Calcium phosphate coatings for bio-implant applications: materials, performance factors, and methodologies. Mater Sci Eng R. 2009;66(1–3):1–70.
8. Liu X, Chu PK, Ding C. Surface modification of titanium, titanium alloys, and related materials for biomedical applications. Mater Sci Eng R. 2004;47(3–4):49–121.
9. Xue W, Tao S, Liu X, Zheng X, Ding C. In vivo evaluation of plasma sprayed hydroxyapatite coatings having different crystallinity. Biomaterials. 2004;25(3):415–21.
10. Hoffmann B, Feldmann M, Ziegler G. Sol–gel and precursor-derived coatings with cover function on medical alloys. J Mater Chem. 2007;17(38):4034–40. doi:10.1039/b707996f.
11. Xiao SJ, Textor M, Spencer ND, Wieland M, Keller B, Sigrist H. Immobilization of the cell-adhesive peptide Arg-Gly-Asp-Cys (RGDC) on titanium surfaces by covalent chemical attachment. J Mater Sci Mater Med. 1997;8(12):867–72. doi:10.1023/a:1018501804943.
12. Erdtmann M, Keller R, Baumann H. Photochemical immobilization of heparin, dermatan sulphate, dextran sulphate and endothelial cell surface heparan sulphate onto cellulose membranes for the preparation of athrombogenic and antithrombogenic polymers. Biomaterials. 1994;15(13):1043–8.
13. Mani G, Chandrasekar B, Feldman MD, Patel D, Agrawal CM. Interaction of endothelial cells with self-assembled monolayers for potential use in drug-eluting coronary stents. J Biomed Mater Res B. 2009;90B(2):789–801. doi:10.1002/jbm.b.31348.
14. Zheludkevich ML, Salvado IM, Ferreira MGS. Sol–gel coatings for corrosion protection of metals. J Mater Chem. 2005;15(48):5099–111. doi:10.1039/b419153f.
15. Wang D, Bierwagen GR. Sol–gel coatings on metals for corrosion protection. Prog Org Coat. 2009;64(4):327–38. doi:10.1016/j.porgcoat.2008.08.010.
16. Ferrer ML, del Monte F, Levy D. A novel and simple alcohol-free sol–gel route for encapsulation of labile proteins. Chem Mater. 2002;14(9):3619–21. doi:10.1021/cm025562r.
17. Reetz MT, Tielmann P, Wiesenhofer W, Konen W, Zonta A. Second generation sol–gel encapsulated lipases: robust heterogeneous biocatalysts. Adv Synth Catal. 2003;345(6–7):717–28. doi:10.1002/adsc.200303016.
18. Sanctis O, Gómez L, Pellegri N, Duran A. Rescubrimientos protectores sobre acero inoxidable producidos por sol–gel. Spain patent. 1993.
19. Sayilkan H, Sener S, Sener E, Sulu M. The sol–gel synthesis and application of some anticorrosive coating materials. Mater Sci. 2003;39(5):733–9.
20. Patel N, Best SM, Bonfield W, Gibson IR, Hing KA, Damien E, Revell PA. A comparative study on the in vivo behavior of hydroxyapatite and silicon substituted hydroxyapatite granules. J Mater Sci Mater Med. 2002;13(12):1199–206. doi:10.1023/a:1021114710076.
21. Gupta R, Kumar A. Bioactive materials for biomedical applications using sol–gel technology. Biomed Mater. 2008;3(3):034005. doi:10.1088/1748-6041/3/3/034005.
22. Reiner T, Kababya S, Gotman I. Protein incorporation within Ti scaffold for bone ingrowth using sol–gel SiO_2 as a slow release carrier. J Mater Sci Mater Med. 2008;19(2):583–9. doi:10.1007/s10856-007-3194-3.
23. Reffitt DM, Ogston N, Jugdaohsingh R, Cheung HFJ, Evans BAJ, Thompson RPH, Powell JJ, Hampson GN. Orthosilicic acid stimulates collagen type 1 synthesis and osteoblastic differentiation in human osteoblast-like cells in vitro. Bone. 2003;32(2):127–35.
24. Hench LL. Stimulation of bone repair by gene activating glasses. In: Barbosa MA, Monteiro FJ, Correia R, Leon B, editors. Bioceramics, vol 16, Key engineering materials, vol 254-2. Zurich-Uetikon: Trans Tech Publications; 2004. p. 3–6.
25. Zolkov C, Avnir D, Armon R. Tissue-derived cell growth on hybrid sol–gel films. J Mater Chem. 2004;14(14):2200–5. doi:10.1039/b401715n.
26. Gallardo J, Galliano P, Duran A. Biactive and protective sol–gel coatings on metals for orthopaedic protheses. J Sol–Gel Sci Technol. 2001;21:65–74.
27. Gallardo J, Galliano P, Moreno R, Duran A. Bioactive sol–gel coatings for orthopaedic prosthesis. J Sol–Gel Sci Technol. 2000;19(1–3):107–11.
28. Munir G, Huang J, Edirisinghe M, Nangrejo R, Bonfield W. Electrohydrodynamic processing of calcium phosphates: coating and patterning for medical implants. Nano Life. 2012;2(1):1250008/1–17. doi:10.1142/S1793984411000426.
29. Munir G, Di Silvio M, Edirisinghe M, Bonfield W, Huang J. A novel surface topographical concept for bone implant. MRS Online Proceedings Library; 2011. p. 1301. doi:10.1557/opl.2011.166.
30. Tsuru K, Robertson Z, Annaz B, Gibson IR, Best SM, Shirosaki Y, Hayakawa S, Osaka A. Sol–gel synthesis and in vitro cell compatibility analysis of silicate-containing biodegradable hybrid gels. Key Eng Mater. 2008;361–363:447–50.
31. Beganskiene A, et al. Modified sol–gel coatings for biotechnological applications. J Phys Conf Ser. 2007;93(1):012050.
32. Almeida RM, Marques AC. Characterization of sol–gel materials by infrared spectroscopy. In: Sumio S, editor. Sol–gel science and technology. Processing, characterization and applications, vol II:

characterization of sol–gel materials and products. Lisboa: Kluwer; 2005. p. 65–89.
33. Innocenzi P, Brusatin G, Guglielmi M, Babonneau F. Structural characterization of hybrid organic–inorganic materials. In: Sumio S, editor. Sol–gel science and technology. Processing, characterization and applications, vol II: characterization of sol–gel materials and products. Lisboa: Kluwer; 2005. p. 139–57.
34. Li Y-S, Wright PB, Puritt R, Tran T. Vibrational spectroscopic studies of vinyltriethoxysilane sol–gel and its coating. Spectrochim Acta A. 2004;60(12):2759–66.
35. Falaize S, Radin S, Ducheyne P. In vitro behavior of silica-based xerogels intended as controlled release carriers. J Am Ceram Soc. 1999;82(4):969–76.
36. Sahin S, Cehreli MC, Yalcin E. The influence of functional forces on the biomechanics of implant-supported prostheses—a review. J Dent. 2002;30(7):271–82.
37. Chang YL, Lew D, Park JB, Keller JC. Biomechanical and morphometric analysis of hydroxyapatite-coated implants with varying crystallinity. J Oral Maxillofac Surg. 1999;57(9):1096–108.
38. Li LH, Kommareddy KP, Pilz C, Zhou CR, Fratzl P, Manjubala I. In vitro bioactivity of bioresorbable porous polymeric scaffolds incorporating hydroxyapatite microspheres. Acta Biomater. 2010;6(7):2525–31. doi:10.1016/j.actbio.2009.03.028.